Lack of P2Y13 in mice fed a high cholesterol diet results in decreased hepatic cholesterol content, biliary lipid secretion and reverse cholesterol transport.

Laeticia Lichtenstein, Nizar Serhan, Wijtske Annema, Guillaume Combes, Bernard Robaye, Jean-Marie Boeynaems, Bertrand Perret, Uwe Tietge, Muriel Laffargue, Laurent Martinez

Nutrition&Metabolism

BRIEF COMMUNICATION Open Access

Lack of $P2Y_{13}$ in mice fed a high cholesterol diet results in decreased hepatic cholesterol content, biliary lipid secretion and reverse cholesterol transport

Laeticia Lichtenstein[1,2†], Nizar Serhan[1,2†], Wijtske Annema[3], Guillaume Combes[1,2], Bernard Robaye[4], Jean-Marie Boeynaems[4], Bertrand Perret[1,5], Uwe J F Tietge[3], Muriel Laffargue[1,2] and Laurent O Martinez[1,2,5*]

Abstract

Background: The protective effect of HDL is mostly attributed to their metabolic function in reverse cholesterol transport (RCT), a process whereby excess cellular cholesterol is taken up from peripheral cells, processed in HDL particles, and later delivered to the liver for further metabolism and biliary secretion. Mechanistically, the purinergic $P2Y_{13}$ ADP-receptor is involved in hepatic HDL endocytosis (i.e., uptake of both HDL protein + lipid moieties), which is considered an important step of RCT. Accordingly, chow-fed $P2Y_{13}$ knockout ($P2Y_{13}^{-/-}$) mice exhibit lower hepatic HDL uptake, which translates into a decrease of hepatic free cholesterol content and biliary cholesterol and phospholipid secretion.

Findings: The aim of this study was to determine the effect of high cholesterol diet (HCD) in $P2Y_{13}^{-/-}$ mice, in order to mimic high dietary cholesterol intake, which is a major cause of dyslipidemia in humans. As previously reported with chow-diet, HCD did not affect plasma lipid levels in $P2Y_{13}^{-/-}$ compared with control mice but decreased hepatic free and esterified cholesterol content ($p < 0.05$, $P2Y_{13}^{-/-}$ versus control). Interestingly, biliary lipid secretion and macrophages-to-feces RCT were more dramatically impaired in $P2Y_{13}^{-/-}$ mice fed a HCD than chow-diet. HCD did not enhance atherosclerosis in $P2Y_{13}^{-/-}$ compared with control mice.

Conclusion: This study demonstrates that high dietary cholesterol intake accentuated the metabolic phenotype of $P2Y_{13}^{-/-}$ mice, with impaired hepatobiliary RCT. Although other animal models might be required to further evaluate the role of $P2Y_{13}$ receptor in atherosclerosis, $P2Y_{13}$ appears a promising target for therapeutic intervention aiming to stimulate RCT, particularly in individuals with lipid-rich diet.

Keywords: $P2Y_{13}$, HDL, HDL-uptake, High cholesterol diet, Bile lipid secretions, Reverse cholesterol transport, Cholesterol metabolism, Liver, ATP synthase

Findings

Introduction/research hypothesis

Dyslipidemia, reflected by either high triglyceride or cholesterol plasma concentrations, is a major risk factor of atherosclerosis [1]. The risk of atherosclerosis, a leading cause of cardiovascular disease and death, is inversely correlated to plasma high-density lipoprotein cholesterol (HDL-C). The protective effect of HDL particles is mostly attributed to their central function in Reverse Cholesterol Transport (RCT), a process whereby peripheral excessive cholesterol, especially that contained in macrophage foam cells, is taken up to be processed in HDL particles, and later delivered to the liver for final excretion into the feces either as neutral sterols or after metabolic conversion into bile acids [2]. This process, which represents a major pathway of the body to eliminate proatherogenic cholesterol, relies on specific interactions between HDL

* Correspondence: Laurent.Martinez@inserm.fr.
†Equal contributors
[1]INSERM, UMR 1048, Institut des Maladies Métaboliques et Cardiovasculaires, Toulouse 31432, France
[2]Université de Toulouse III, UMR 1048, Toulouse 31300, France
Full list of author information is available at the end of the article

particles and cells, both peripheral (cholesterol efflux) and hepatic cells (cholesterol output). We recently identified a new pathway for holoparticle HDL endocytosis by the liver (i.e., hepatic uptake of both HDL protein + lipid moieties), involved in RCT. In this pathway, apoA-I, the major protein of HDL, binds an ecto-F_1-ATPase leading to ATP hydrolysis into ADP [3]. Extracellular ADP activates the purinergic $P2Y_{13}$ ADP-receptor, which stimulates *in fine* HDL uptake through an unknown low affinity receptor, distinct from the classical HDL receptor, SR-BI. Our recent work has confirmed the role of the $P2Y_{13}$ receptor in HDL-mediated RCT *in vivo* [4]. We showed that $P2Y_{13}$-deficient mice ($P2Y_{13}^{-/-}$) exhibited a decrease in hepatic HDL uptake, hepatic cholesterol content, and biliary cholesterol output, although their plasma HDL-C and other lipid levels were normal. These metabolic changes translated into a substantial decrease in the rate of macrophage-to-feces RCT. Therefore, key features of RCT were impaired in $P2Y_{13}^{-/-}$ mice.

In order to investigate the role of $P2Y_{13}$ in a dyslipidemic context, we studied the phenotype of $P2Y_{13}^{-/-}$ mice fed high cholesterol diet (HCD) for 16 weeks. Our results show that chronically increased cholesterol intake accentuates the metabolic phenotype of $P2Y_{13}^{-/-}$ mice, with impaired hepatobiliary metabolism. Specifically, (i) hepatic HDL uptake mediated by $P2Y_{13}$ receptor plays an important role in regulating liver cholesterol content, (ii) $P2Y_{13}$ receptor is essential for normal biliary lipid secretion and fecal excretion of cholesterol originating from macrophages, (iii) these effects of $P2Y_{13}$ activity on the flux of HDL toward the liver does not affect HDL-C level per se or selected HDL functions. Overall, this work emphasizes the essential role of $P2Y_{13}$ in RCT in a dyslipidemic context.

Materials and methods

Animals and diets

The animals were caged in an animal facility with alternating 12 h periods of light (07:00 am-7:00 pm) and dark (7:00 pm-07:00 am). 8 week-old male $P2Y_{13}^{-/-}$ and $P2Y_{13}^{+/+}$ littermates mice (C57BL/6 background) were fed for 16 weeks a high cholesterol diet (Harlan TD 96335, 1.25% cholesterol) then used for experimentation. All animal procedures were in accordance with the guidelines of the Committee on Animals of the Midi-Pyrénées Ethics Committee on Animal Experimentation and with the French Ministry of Agriculture license.

Plasma lipoprotein analyses

Plasma samples were collected at 11 am, after a fasting period of 3 h. Total cholesterol and triglycerides were measured with commercial kits (CHOD-PAP for cholesterol and GPO-PAP for triglycerides; BIOLABO SA, Maizy, France). Quantification of plasma lipoproteins was performed using an Ultimate® 3000 HPLC system (Dionex, USA) as previously described [5].

Hepatic lipid analyses

Hepatic cholesterol and triglycerides were analyzed, following Bligh & Dyer lipid extraction, by gas–liquid chromatography, as previously described [4].

Cannulation of the common bile duct and bile lipid analysis

Mice were fasted for 3 hours and were then anesthetized by intra-peritoneal injection of ketamine hydrochloride and xylazine hydrochloride. At 11 am, gallbladder was cannulated and bile was harvested for 30 minutes, after a stabilization time of 30 minutes. Bile acid, phospholipid and cholesterol analysis was performed as previously reported [5].

In vivo macrophage-to-feces RCT

RCT assay was performed as previously described [4]. Briefly, thioglycollate-elicited mouse peritoneal macrophages, harvested from C57BL/6(J) donor mice, were loaded for 24 hours with 50 μg/mL acetylated LDL and 5 μCi / ml ^{3}H-cholesterol, then injected intraperitoneally in recipient mice (two million dpm/mouse). Blood samples were taken 6, 24 and 48 hours after macrophages injection, feces were collected continuously for 48 hours and livers were harvested 48 hours after macrophages injection and stored at −80°C until lipid extraction and radioactivity counting [4]. All counts were expressed as a percentage of the administered tracer dose.

Table 1 Plasma lipid values in $P2Y_{13}^{+/+}$ (WT) and $P2Y_{13}^{-/-}$ mice fed a HCD for 16 weeks

	VLDL		LDL		HDL	
	WT	$P2Y_{13}^{-/-}$	WT	$P2Y_{13}^{-/-}$	WT	$P2Y_{13}^{-/-}$
TC (mg/dl)	14.1 ± 1.92	12.2 ± 3.42	25.1 ± 1.31	18.5 ± 0.34	85.01 ± 16.9	90.62 ± 8.88
FC (mg/dl)	4.55 ± 0.71	3.31 ± 0.76	10.3 ± 4.57	6.00 ± 0.20	33.58 ± 2.56	29.45 ± 2.80
EC (mg/dl)	9.86 ± 1.48	8.93 ± 2.65	14.8 ± 3.06	12.5 ± 0.29	53.33 ± 14.2	61.49 ± 6.1
TG (mg/dl)	24.6 ± 1.27	23.5 ± 4.52	7.26 ± 1.05	9.43 ± 1.66	6.75 ± 2.23	2.45 ± 0.27

Values are expressed as means ± SEM; n = 4 mice per group.

Table 2 Hepatic lipid values in $P2Y_{13}^{+/+}$ (WT) and $P2Y_{13}^{-/-}$ mice fed a HCD for 16 weeks

	WT	$P2Y_{13}^{-/-}$
Total cholesterol (nmol/mg)	67.11 ± 3.84	50.50 ± 2.53*
Free cholesterol (nmol/mg)	13.28 ± 0.96	9.65 ± 0.54*
Esterified cholesterol (nmol/mg)	53.41 ± 3.37	41.97 ± 1.89*
Triglycerides (nmol/mg)	30.69 ± 3.76	29.59 ± 2.16

Values are expressed as means ± SEM; n = 10 mice per group.
*Indicates significant difference ($p < 0.05$) from control mice.

Hepatic gene expression

Liver and whole intestine RNA isolation, reverse transcription and real-time quantitative PCR analysis were performed as previously described [5].

HDL functionality

HDL were isolated from mouse plasma, after precipitation of apoB-containing lipoproteins with polyethylene glycol-6000 [6]. Anti-oxidative property of HDL was assessed by measuring the capacity of HDL to inhibit the oxidation of native LDL as previously described [6,7]. Anti-inflammatory property of HDL was evaluated on human umbilical vein endothelial cells (HUVECs) by measuring MCP-1 gene expression as previously described [6]. Efflux experiments were performed by measuring cholesterol efflux for 5 hours from primary mouse peritoneal macrophages towards either plasma (1%, v/v) or apoB-depleted lipoproteins (2%, v/v), as previously described [6].

Aortic sinus quantification

The lesions were estimated according to Paigen and collaborators [8] Briefly, each heart was frozen on a cryostat mount with OCT compound (Tissue-Tek), and stored at −80°C. Hearts were cut using a Leica CM3050S cryostat. Fifty sections of 10-μm thickness were prepared from the top of the left ventricle, where the aortic valves were first visible, up to a position in the aorta where the valve cusps were just disappearing from the field. After drying for 1 hour, the sections were stained with oil red O and counterstained with Mayer's hematoxylin. Five sections out of the 50, each separated by 100 μm, were used for specific morphometric evaluation of intimal lesions using a computerized Leica image analysis system, consisting of a Leica DMRE microscope coupled to a video camera and Leica Qwin Imaging software (Leica Ltd, Cambridge, UK). The first and most proximal section to the heart was taken 100 μm distal to the point where the aorta first becomes rounded. Lipid droplets <500 μm^2 as well as those located in the media were excluded from the measurements. The

Table 3 Biliary lipid values in $P2Y_{13}^{+/+}$ (WT) and $P2Y_{13}^{-/-}$ mice fed a HCD for 16 weeks

	WT	$P2Y_{13}^{-/-}$
Bile flow (μl/min/100 g BW)	5.58 ± 0.42	4.35 ± 0.26*
Cholesterol secretion (nmol/min/100 g BW)	3.79 ± 0.27	2.71 ± 0.36*
Bile acid secretion (nmol/min/100 g BW)	209.9 ± 16.0	167.1 ± 10.2*
Phospholipid secretion (nmol/min/100 g BW)	15.7 ± 0.2	9.7 ± 0.2*

Values are expressed as means ± SEM; n = 10 mice per group.
*Indicates significant difference ($p < 0.05$) from control mice.

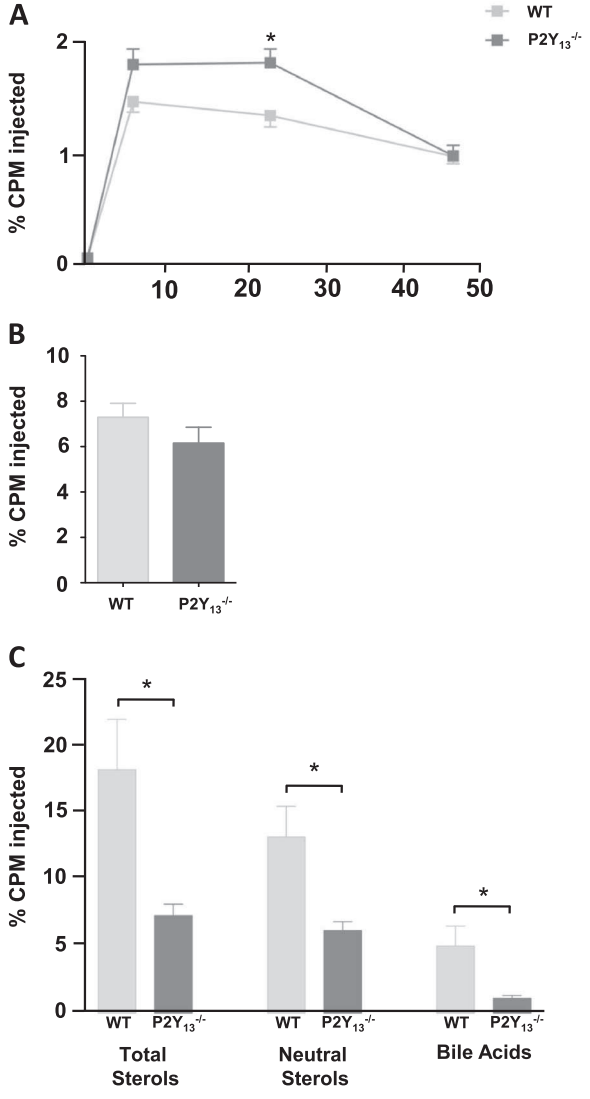

Figure 1 Lack of $P2Y_{13}$ in mice fed HCD decreases *in vivo* macrophage-to-feces reverse cholesterol transport. Two million of ^{3}H-cholesterol–labeled peritoneal macrophages from C57BL/6 donor mice were injected intraperitoneally in $P2Y_{13}^{-/-}$ (dark grey squares and bars) and WT (light gray squares and bars) mice fed HCD. **(A)** ^{3}H-cholesterol appearance in plasma 6, 24, and 48 hours after macrophage administration. **(B)**, ^{3}H-cholesterol tracer recovery within liver 48 hours after macrophages injection. **(C)**, ^{3}H-cholesterol appearance in feces collected continuously from 0 to 48 hours, after macrophages injection. Data are expressed as percent cpm injected ± SEM; n = 6 mice group. Statistically significant differences from WT mice are indicated as *$p < 0.05$.

Table 4 Effect of HCD in $P2Y_{13}^{-/-}$ mice on hepatic mRNA expression of genes involved in lipid homeostasis

Gene		Fold-change	Accession N°	Gene title
Scarb1	1.00 ± 0.12	0.86 ± 0.10 (p = 0.67)	NM_016741	Scavenger receptor class B, member 1
Ldlr	1.00 ± 0.17	1.02 ± 0.15 (p = 0.75)	NM_010700	Low density lipoprotein receptor
Abca1	1.00 ± 0.16	**0.59 ± 0.05*** (p = 0.04)	NM_013454	ATP-binding cassette, sub-family A, member 1
Abcg1	1.00 ± 0.10	**0.68 ± 0.07*** (p = 0.02)	NM_009593	ATP-binding cassette, sub-family G, member 1
Apoa1	1.00 ± 0.10	0.97 ± 0.07 (p = 0.72)	NM_009692	Apolipoprotein A-I
Cyp7a1	1.00 ± 0.23	1.61 ± 0.24 (p = 0.06)	NM_007824	Cytochrome P450, family 27, subfamily A, polypeptide 1
Cyp27a1	1.00 ± 0.13	1.11 ± 0.13 (p = 0.53)	NM_024264	Cytochrome P450, family 8, subfamily B, polypeptide 1
Cyp8b1	1.00 ± 0.22	1.64 ± 0.26 (p = 0.18)	NM_010012	Cytochrome P450, family 8, subfamily B, polypeptide 1
Abcg5	1.00 ± 0.12	**0.64 ± 0.05*** (p = 0.03)	NM_031884	ATP-binding cassette, sub-family G, member 5
Abcg8	1.00 ± 0.10	**0.61 ± 0.07**** (p = 0.003)	NM_026180	ATP-binding cassette, sub-family G, member 8
Abcb4	1.00 ± 0.07	0.74 ± 0.08 (p = 0.06)	NM_008830	ATP-binding cassette, sub-family G, member 4
Abcb11/Bsep	1.00 ± 0.11	1.33 ± 0.10 (p = 0.22)	NM_021022	ATP-binding cassette, sub-family B (MDR/TAP), member 11
Ntcp/Slc10a1	1.00± 0.22	1.51 ± 0.17 (p = 0.11)	NM_011387	Solute carrier family 10 (sodium/bile acid cotransporter family), member 1
Oatp/Slco1a1	1.00 ± 0.16	1.33 ± 0.19 (p = 0.47)	NM_013797	Solute carrier organic anion transporter family, member 1A2
Hmgcr	1.00 ± 0.01	1.02 ± 0.09 (p = 0.44)	NM_008255	3-hydroxy-3-methylglutaryl-Coenzyme A reductase
Srebp2	1.00 ± 0.09	0.74 ± 0.07 (p = 0.06)	NM_033218	Sterol regulatory element binding transcription factor 2

Real-time PCR was performed on individual livers of 3 h fasted mice (n = 10 mice per group). For all genes, the fold change was calculated by dividing the $P2Y_{13}^{-/-}$ mice value by the wild-type mice value (e.g. an increase of 80% from wild-type is reported as 1.80). * and ** indicate significant difference ($p < 0.05$ and $p < 0.01$ respectively) from wild-type mice.

mean lesion size (expressed in μm^2) in these 5 sections was used to evaluate the lesion size of each animal. The coded slides were examined blind in two separate analyses by the same examiner and gave consistent results (r = .97).

Statistical analysis

All results are presented as means ± SEM. Comparisons between groups were made using the Mann–Whitney test for independent samples. Outcomes of $p < 0.05$ were considered significant. Analyses were performed using GraphPad Prism 6 software.

Results and discussion

In order to investigate the role of $P2Y_{13}$ receptor in a dyslipidemic context, we studied the phenotype of $P2Y_{13}^{-/-}$ mice fed high cholesterol diet (HCD) for 16 weeks. Body weight and liver weight were unchanged between $P2Y_{13}^{-/-}$ and wild-type (WT, C57BL/6) mice maintained on HCD (data not shown) and plasma total cholesterol, HDL-C, LDL-C and triglycerides did not differ either (Table 1). However, on HCD feeding, hepatic total cholesterol content was significantly lower in $P2Y_{13}^{-/-}$ than in WT mice, with decrease in both cholesterol ester and free cholesterol (Table 2). To further assess the effect of HCD on the metabolic phenotype of $P2Y_{13}^{-/-}$ mice, we measured biliary flow and lipid secretion, which is considered an essential step in RCT [9]. As reported in Table 3, biliary flow was significantly decreased and biliary secretion of cholesterol, bile acid and phospholipid were also significantly reduced in $P2Y_{13}^{-/-}$ as compared to WT mice after

Table 5 Effect of HCD in $P2Y_{13}^{-/-}$ mice on intestinal mRNA expression of genes involved in lipid homeostasis

Gene		Fold-change	Accession N°	Gene title
Npc1l1	1.00 ± 0.21	1.39 ± 0.21 (p = 0.36)	NM_207242	Niemann-Pick C1-like protein 1
Abcg5	1.00 ± 0.26	1.53 ± 0.24 (p = 0.36)	NM_026180	ATP-binding cassette, sub-family G, member 5
Abcg8	1.00 ± 0.21	1.47 ± 0.19 (p = 0.18)	NM_026180	ATP-binding cassette, sub-family G, member 8
AbcA1	1.00 ± 0.15	1.52 ± 0.23 (p = 0.18)	NM_013454	ATP-binding cassette, sub-family A, member 1
Abcg1	1.00 ± 0.22	0.89 ± 0.11 (p = 0.94)	NM_009593	ATP-binding cassette, sub-family G, member 1
Scarb1	1.00 ± 0.25	1.41 ± 0.32 (p = 0.73)	NM_016741	Scavenger receptor class B, member 1
Oatp/Slco1a1	1.00 ± 0.41	0.81 ± 0.17 (p = 0.94)	NM_013797	Solute carrier organic anion transporter family, member 1A2
Fgf15	1.00 ± 0.28	1.09 ± 0.27 (p = 0.94)	NM_008003	Fibroblast growth factor 15

Real-time PCR was performed on individual intestine of 3 h fasted mice (n = 6 mice per group). For all genes, the fold change was calculated by dividing the $P2Y_{13}^{-/-}$ mice value by the wild-type mice value (e.g. an increase of 80% from wild-type is reported as 1.80).

16 weeks of HCD. We next measured the movement of ^{3}H-cholesterol from macrophages to the feces, which is a surrogate well-established method to evaluate *in vivo* RCT [10]. We observed that macrophage-to-feces RCT was impaired in $P2Y_{13}^{-/-}$ as compared to WT mice, as reflected by a ~60% reduction of total sterol recovered in feces (Figure 1C, -53±5 and –78±4 in % of neutral sterols and bile acids, respectively). This reduced RCT is most likely attributable to the described function of $P2Y_{13}$ receptor in hepatic HDL uptake [4,11]. Accordingly, $P2Y_{13}^{-/-}$ mice fed HCD displayed a significant higher ^{3}H- tracer present in plasma at 6 and 24 h (Figure 1A) and a trend to lower ^{3}H-tracer recovered in the liver at 48 h, as compared to WT mice (Figure 1B). Macrophage-to-feces RCT experiments have frequently reported that ^{3}H-tracer recovered in feces is more sensitive to evidence

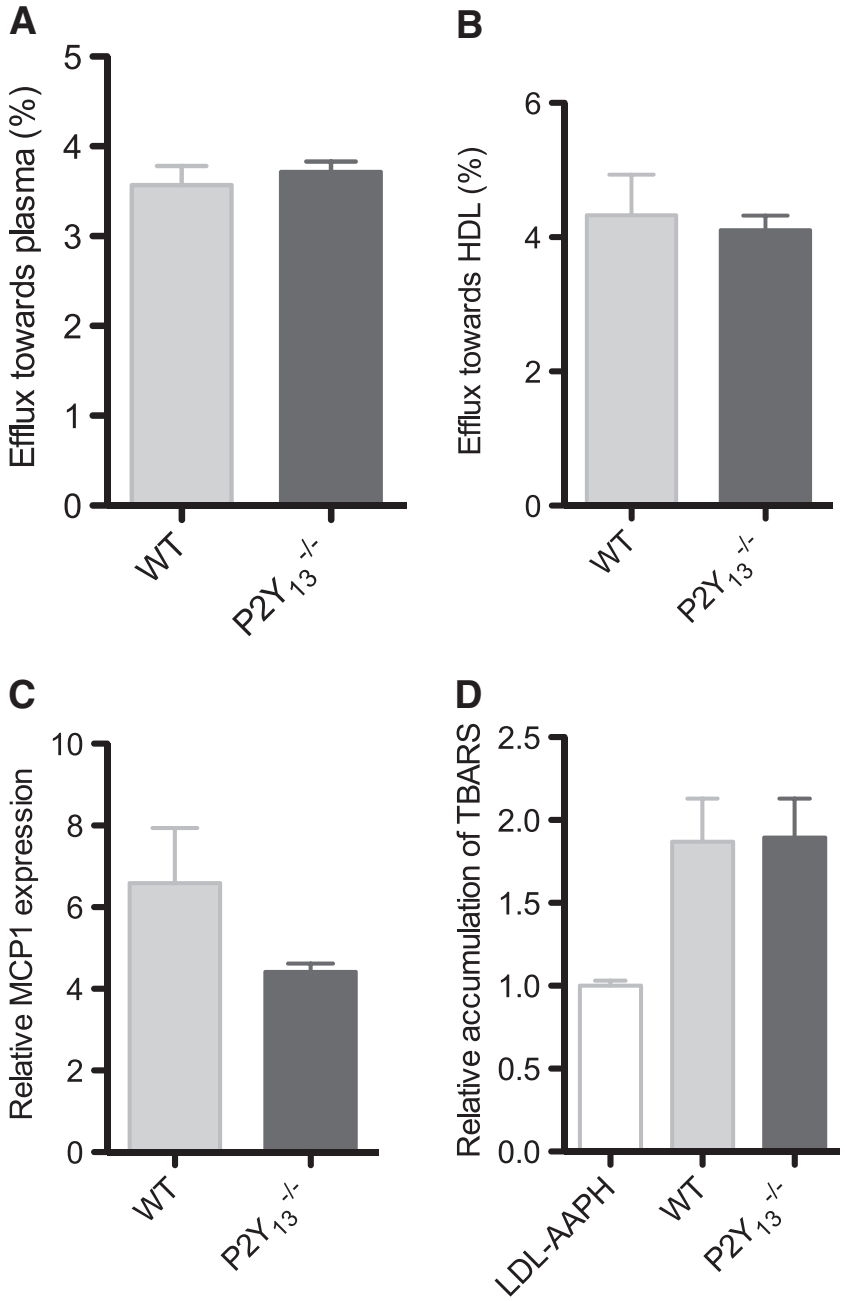

Figure 2 $P2Y_{13}$ deficiency does not change the functional properties of HDL on HCD. HDL function was determined as cholesterol efflux **(A and B)**, protection of HUVECs against inflammation **(C)**, protection of LDL against oxidation **(D)**. Data are presented as means ± SEM, n = 10 mice per group. TBARS: Thiobarbituric aid reactive substances.

changes in RCT than ^{3}H-tracer present in plasma and liver which is often unchanged [10,12], probably because radioactivity recovered in feces represents the endpoint of RCT whereas radioactivity present in plasma and liver depends on cholesterol flux of a freely distributable tracer. This hence might explain the unchanged % of ^{3}H-tracer present in plasma at 48 h and the lack of a significance in the decrease of ^{3}H-tracer in the liver of $P2Y_{13}^{-/-}$ compared to WT mice (Figure 1A, B).

$P2Y_{13}$ deficiency results in a ~40% decrease of hepatic messenger RNA (mRNA) expression of the heterodimeric ATP-binding transporter Abcg5 and Abcg8 (Table 4), suggesting that the cholesterol derived from HDL that has been internalized through $P2Y_{13}$ receptor might use the Abcg5/g8 dependent pathway for apical biliary cholesterol secretion [13]. Hepatic gene expression of the other transporters controlling bile acid and phospholipid fluxes in the liver, such as biliary phospholipid transport protein (Abcb4/mdr3), bile salt export pump (Abcb11/bsep), basolateral transporter sodium taurocholate cotransporting polypeptide (Ntcp) and organic anion transport polypeptide (Oatp) were unchanged (Table 4). As reported in Tables 4 and 5, there was also no significant change in the expression of gene controlling bile acid production such as hepatic cholesterol 7 alpha-hydroxylase (Cyp7A1), hepatic sterol 27-hydroxylase (Cyp27A1), hepatic sterol 12-alpha-hydroxylase (Cyp8b1) and intestinal Fibroblast growth factor 15 (Fgf15). Furthermore, the reduction of bile acid secretion observed in $P2Y_{13}^{-/-}$ mice compared to WT mice was mainly driven by lower bile flow (Table 3) since the concentration of bile acid in bile was not significantly reduced (data not shown) whereas both secretion and concentration of biliary cholesterol and phospholipid were decreased (Table 3 and data not shown). Altogether these data indicate that the effect of $P2Y_{13}$ deficiency on decreasing bile acid secretion into the bile cannot be attributed to a decrease of hepatic bile acids synthesis or apical transport but is more likely driven by the decrease of biliary flow. However, further investigation is required to determine the mechanism by which $P2Y_{13}$-mediated HDL endocytosis regulates biliary lipid secretion process. Indeed, although recent studies evidenced that HDL internalized by hepatocytes are transported to two intracellular pools – a rapid turnover retroendocytic pool involving endosomal recycling compartment (ERC) and a slow-turnover pool, involving multivesicular bodies, that is eventually further transported to lysosomes for degradation [14], the process by which intracellular HDL trafficking governs biliary lipid secretion is still poorly characterized.

Interestingly, hepatic mRNA expression of Abca1 and Abcg1, which contribute to cellular cholesterol efflux towards lipid-poor ApoA-I and HDL particles, respectively [13], was significantly decreased in $P2Y_{13}^{-/-}$ mice after 16 weeks of HCD (Table 4). These results might suggest that the decrease of hepatobiliary cholesterol secretion observed in $P2Y_{13}^{-/-}$ mice fed a HCD is associated with a decrease of *de novo* HDL formation, thus explaining the unchanged plasma HDL-C levels *per se*, as previously proposed for $P2Y_{13}^{-/-}$ mice fed a chow diet [4]. Alternatively, the $P2Y_{13}$-mediated HDL endocytosis pathway might efficiently drive cholesterol from HDL towards biliary lipid secretion but could be quantitatively negligible regarding the steady state concentration of plasma HDL-C. Accordingly, it is now well established that macrophage-derived cholesterol represents only a minor proportion of the total cholesterol transported by HDL particles but is essential to prevent foam cell formation [15] supporting the concept that the dynamics of HDL particles are essential for RCT but not necessary correlated to the static measure of plasma HDL-C concentration.

To assess HDL functionality in these mice, we tested whether $P2Y_{13}$ deletion would influence HDL functionalities regarding either their anti-inflammatory or anti-oxidative properties, or their capacity to elicit efflux from cholesterol-loaded macrophages. However, $P2Y_{13}$-deficient mice did not show any change in these respective HDL functionalities after 16 weeks of HCD (Figure 2), suggesting that $P2Y_{13}$ deletion neither interferes with HDL pleiotropic functions, nor HDL-mediated efflux from cholesterol-loaded macrophages. Furthermore, feeding the HCD for 16 weeks did not result in an increased lipid deposition in the aortic sinus of $P2Y_{13}^{-/-}$ compared to WT mice (Figure 3). Not surprisingly, these results indicate that $P2Y_{13}$ deletion in C57BL/6 mice does not initiate atherosclerosis development. To formally assess the hypothesis whether $P2Y_{13}$ receptor plays a role in atherosclerosis development, mice lacking $P2Y_{13}$ would have to be crossed with a proatherogenic mouse model.

We previously demonstrated that chow-fed $P2Y_{13}$ deficient mice displayed a reduced uptake of HDL by the liver associated to decreased hepatic free cholesterol content and impaired biliary secretion of cholesterol and phospholipids [4]. These metabolic changes translated into a substantial ~45% decrease in the rate of macrophage-to-

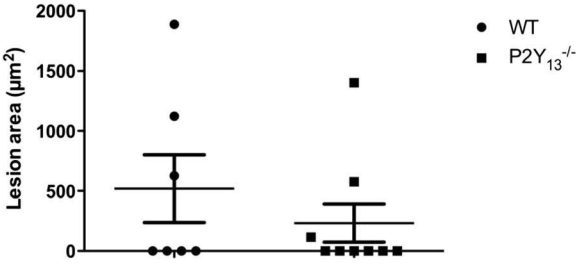

Figure 3 $P2Y_{13}$ deficiency does not induce atherosclerosis development on HCD. Aortic sinus sections were stained with oil red O and lipid content was quantified. Data are presented as means ± SEM, n = 6 in WT group, and n = 9 in $P2Y_{13}^{-/-}$ group.

feces RCT [4]. In the present study, we observed that a chronic high cholesterol intake accentuates this metabolic phenotype, with a more dramatic impaired hepatobiliary RCT. Indeed, using HCD-fed $P2Y_{13}^{-/-}$ compared to WT mice, we reported here that both free and esterified cholesterol content in the liver were decreased (Table 2), together with biliary flow and biliary lipid secretion (Table 3) and a ~60% reduction in the rate of macrophage-to-feces RCT (Figure 1).

$P2Y_{13}$ receptor is also expressed in the intestine [16] and could potentially also regulate intestinal cholesterol absorption or excretion. Our results indicates that the mRNA expression level of the principal genes involved in cholesterol absorption were unchanged between $P2Y_{13}^{-/-}$ and WT mice maintained on HCD (Table 5), suggesting that cholesterol absorption is unchanged in $P2Y_{13}^{-/-}$ mice.

Overall, our work emphasizes the importance of hepatic $P2Y_{13}$ activity when diet is rich in cholesterol, by regulating biliary lipid output and overall RCT without affecting HDL-C level *per se* or selected HDL functions. Thus, this study opens the way to reconsider pharmacological approaches to target HDL metabolism, particularly with regard to mechanistic aspects of RCT, by improving the flux of circulating HDL towards the liver (e.g., by stimulating $P2Y_{13}$) rather than increasing plasma HDL-C levels.

Abbreviations

HDL: High density Lipoprotein; LDL: Low density lipoprotein; ApoA-I: apolipoprotein A-I; HCD: High cholesterol diet; RCT: Reverse cholesterol tansport; Ecto-F_1ATPase: Ectopic F_1-ATPase; ATP: Adenosine triphosphate; ADP: Adenosine diphosphate; Abca1: ATP binding cassette subfamily A member 1; Abcb4: ATP binding cassette subfamily B member 4; Abcg1: ATP binding cassette subfamily G member 1; Abcg5: ATP binding Cassette subfamily G member 5; Abcg8: ATP binding Cassette subfamily G member 8; Oatp: Organic anion transport polypeptide; Ntcp: Sodium taurocholate cotransporting polypeptide; WT: Wild-type; EC: Esterified cholesterol; FC: Free cholesterol; TC: Total cholesterol.

Competing interests

The authors declare that they have no competing of interest.

Authors' contributions

LOM conceived the study and participated in its design and coordination. BR and JMB conceived $P2Y_{13}$ knockout mice and participated in the design of the study. LL, NS and GC carried out animal metabolic studies and participated in the design of the study. WA and UJFT carried out HDL functionality assays and analyzed the data. LOM, LL and NS have interpreted the overall data and drafted the manuscript. BP and ML revised the manuscript critically for important intellectual content. All authors read and approved the final manuscript.

Acknowledgments

We thank the technical service of the animal facility (Genotoul Anexplo Platform, Toulouse). We thank J. Bertrand-Michel and V. Roques (MetaToul-Lipidomic Core Facility INSERM UMR 1048, France, part of Toulouse Metatoul Plateform) and Eric Lacoste (Synelvia, Prologue Biotech, Labège, France) for lipidomic analysis, advice and technical assistance.

Funding

This study was supported by the National Research Agency (ANR Emergence and GENO #102 01) and the Midi-Pyrénées Region. LL is a recipient of the Marie Curie IEF fellowship.

Author details

[1]INSERM, UMR 1048, Institut des Maladies Métaboliques et Cardiovasculaires, Toulouse 31432, France. [2]Université de Toulouse III, UMR 1048, Toulouse 31300, France. [3]Department of Pediatrics, University of Groningen, University Medical Center Groningen, Groningen, Netherlands. [4]Institute of Interdisciplinary Research, IRIBHM, Université Libre de Bruxelles, Gosselies, Belgium. [5]CHU de Toulouse, Hôpital Purpan, Toulouse, France.

Received: 24 July 2013 Accepted: 30 October 2013
Published: 6 November 2013

References

1. Pöss J, Custodis F, Werner C, Weingärtner O, Böhm MLU: **Cardiovascular disease and dyslipidemia: beyond LDL.** *Curr Pharm Des* 2011, **17:**861–870.
2. DeGoma EM, DeGoma RL, Rader DJ: **Beyond high-density lipoprotein cholesterol levels evaluating high-density lipoprotein function as influenced by novel therapeutic approaches.** *J Am Coll Cardiol* 2008, **51:**2199–2211.
3. Martinez LO, Jacquet S, Esteve JP, Rolland C, Cabezon E, Champagne E, *et al*: **Ectopic beta-chain of ATP synthase is an apolipoprotein A-I receptor in hepatic HDL endocytosis.** *Nature* 2003, **421:**75–79.
4. Fabre AC, Malaval C, Ben Addi A, Verdier C, Pons V, Serhan N, *et al*: **P2Y13 receptor is critical for reverse cholesterol transport.** *Hepatology* 2010, **52:**1477–1483.
5. Serhan N, Cabou C, Verdier C, Lichtenstein L, Malet N, Perret B, *et al*: **Chronic pharmacological activation of P2Y13 receptor in mice decreases HDL-cholesterol level by increasing hepatic HDL uptake and bile acid secretion.** *Biochim Biophys Acta* 2013, **1831:**719–725.
6. Dullaart RPF, Annema W, de Boer JF, Tietge UJF: **Pancreatic β-cell function relates positively to HDL functionality in well-controlled type 2 diabetes mellitus.** *Atherosclerosis* 2012, **222:**567–573.
7. Nijstad N, de Boer JF, Lagor WR, Toelle M, Usher D, Annema W, *et al*: **Overexpression of apolipoprotein O does not impact on plasma HDL levels or functionality in human apolipoprotein A-I transgenic mice.** *Biochim Biophys Acta* 2011, **1811:**294–299.
8. Paigen B, Morrow A, Holmes PA, Mitchell DWR: **Quantitative assessment of atherosclerotic lesions in mice.** *Atherosclerosis* 1987, **68:**231–240.
9. Nijstad N, Gautier T, Briand F, Rader DJ, Tietge UJF: **Biliary sterol secretion is required for functional in vivo reverse cholesterol transport in mice.** *Gastroenterology* 2011, **140:**1043–1051.
10. Naik SU, Wang X, Da Silva JS, Jaye M, Macphee CH, Reilly MP, *et al*: **Pharmacological activation of liver X receptors promotes reverse cholesterol transport in vivo.** *Circulation* 2006, **113:**90–97.
11. Jacquet S, Malaval C, Martinez LO, Sak K, Rolland C, Perez C, *et al*: **The nucleotide receptor P2Y13 is a key regulator of hepatic high-density lipoprotein (HDL) endocytosis.** *Cell Mol Life Sci* 2005, **62:**2508–2515.
12. François B, Snehal U, Naik Llia F, John S, Millar C, Colin M, Max W, Jeffrey B, George Rothblat DJ: **Both the Peroxisome Proliferator-Activated Receptor δ Agonist, GW0742, and Ezetimibe Promote Reverse Cholesterol Transport in Mice by Reducing Intestinal Reabsorption of HDL-Derived Cholesterol.** *Clin Transl Sci* 2009, **2:**127–133.
13. Dikkers A, Freak De Boer J, Annema W, Groen AK, Tietge UJF: **Scavenger receptor BI and ABCG5/G8 differentially impact biliary sterol secretion and reverse cholesterol transport in mice.** *Hepatology* 2013, **58:**293–303.
14. Röhrl C, Pagler TA, Ellinger A, Pavelka M, Meisslitzer-ruppitsch C: **Europe PMC Funders Group Characterization of endocytic compartments after holo-high density lipoprotein particle uptake in HepG2 cells.** *Histochem Cell Biol* 2011, **133:**261–272.
15. Haghpassand M, Bourassa PK, Francone OL, Aiello RJ: **Monocyte/macrophage expression of ABCA1 has minimal contribution to plasma HDL levels.** *J Clin Invest* 2001, **108:**1315–1320.
16. Communi D, Gonzalez NS, Detheux M, Brezillon S, Lannoy V, Parmentier M, *et al*: **Identification of a novel human ADP receptor coupled to G(i).** *J Biol Chem* 2001, **276:**41479–41485.

doi:10.1186/1743-7075-10-67
Cite this article as: Lichtenstein *et al.*: Lack of $P2Y_{13}$ in mice fed a high cholesterol diet results in decreased hepatic cholesterol content, biliary lipid secretion and reverse cholesterol transport. *Nutrition & Metabolism* 2013 **10**:67.